

Photoabsorption Spectra of Na_n^+ Clusters: Thermal Line-Broadening Mechanisms

M. Moseler,^{1,2} H. Häkkinen,² and Uzi Landman²

¹*Theoretische Quantendynamik, Fakultät für Physik, Universität Freiburg, 79106 Freiburg, Germany*

²*School of Physics, Georgia Institute of Technology, Atlanta, Georgia 30332-0430*

(Received 2 April 2001; published 13 July 2001)

Photoabsorption cross sections of small sodium cluster cations (Na_n^+ , $n = 3, 5, 7,$ and 9) were calculated at various temperatures with the time-dependent local-density approximation in conjunction with *ab initio* molecular dynamics simulations, yielding spectra that agree with measured ones without *ad hoc* line broadening or renormalization. Three thermal line-broadening mechanisms are revealed: (I) lifting of level degeneracies caused by symmetry-breaking ionic motions, (II) oscillatory shifts of the entire spectrum caused by breathing vibrations, and (III) cluster structural isomerizations.

DOI: 10.1103/PhysRevLett.87.053401

PACS numbers: 36.40.Vz, 31.15.Ar, 36.40.Mr

Optical spectroscopy provides invaluable insights into the electronic structure, ionic configurations, thermal processes and dynamics in metal clusters, as well as about the size-dependent evolution of these properties. Indeed, investigations of these issues have been pursued rather intensively for over a decade both experimentally with photodepletion spectroscopy [1,2] and theoretically [3–9] with the main methodology employing the time-dependent local-density approximation (TDLDA) [3,5,10] in conjunction with either jellium models [3–5] (including allowance for shape deformations), where the ionic background is smeared out uniformly, or with electronic structure calculations of various degrees of sophistication where the discrete nature of the ions is incorporated accurately [7,8] or perturbatively [9]. While valuable information pertaining to the optical excitations and damping mechanisms in metal clusters has been obtained through such studies, including the sensitivity of optical features to cluster geometries, a first-principles theoretical description of the optical line shapes, the absolute absorption cross sections, the relevant microscopic line-broadening mechanisms, and their thermal variations, is lacking. This is reflected in the common *ad hoc* employment of line broadening through convolution of spectral lines calculated for selected static cluster configurations with Gaussian or Lorentzian functions [3–5,7,8], or (multiplicative) renormalization of the calculated spectra to the measured ones [9,11].

In this Letter, we demonstrate that photoabsorption cross sections, $\sigma(\omega)$, calculated via the TDLDA along finite temperature Born-Oppenheimer (BO) local-spin-density (LSD) molecular dynamics (MD) (BO-LSD-MD [12]) phase-space trajectories, provide a *quantitative ab initio description* of the *absolute magnitudes, peak positions, and line shapes* of optical absorption spectra measured at various temperatures from Na_n^+ ($n = 3, 5, 7,$ and 9) clusters [2]. An analysis of the results, and in particular the temporal correlations between the calculated $\sigma^t(\omega)$ (where the superscript denotes the value at instant t) and the dynamically evolving cluster configurations, reveals three thermally induced mechanisms which govern the

spectral characteristics: (I) symmetry breaking of the optimal (0 K) cluster geometries due to thermal ionic motion, leading to lifting of electronic level degeneracies and resulting in splitting (fragmentation) of spectral lines; (II) symmetry-conserving breathing motions that modulate the effective density, resulting in oscillatory frequency shifts of the entire spectrum (“spectral sweeping”) that influence the optical absorption peak positions and linewidth; (III) opening of the accessible configurational space, resulting in structural isomerization and consequent electronic structure and spectral variations. The first two mechanisms are operative for smaller clusters (Na_3^+ and Na_5^+) even at relatively low temperatures (e.g., 100 K), while all three occur for the larger ones. The thermal dependence of the spectral characteristics is analyzed, resulting in remarkable first-principles agreement between the calculated and measured $\sigma(\omega)$.

The Kohn-Sham (KS) equations with generalized gradient corrections (GGA) [13] and nonlocal pseudopotentials [14] were solved for Na_n^+ clusters ($n = 3, 5, 7,$ and 9), and based on the Hellmann-Feynman forces, finite temperature trajectories were generated by Langevin dynamics through the use of the BO-LSD-MD (with GGA) method [12]. For each cluster size, starting from the (presumed [7]) GGA-optimized ground state (GS) geometry and an equilibration of 10 ps duration, the system was allowed to evolve dynamically at the prescribed temperature for an additional period of $t_s = 10$ ps. At each instant t , the excitation energies ω_l^t were determined by solving the TDLDA eigenvalue problem [10]

$$\sum_{kl} \left[(\epsilon_{ij}^t)^2 \delta_{ik} \delta_{jl} + 4\sqrt{\epsilon_{ij}^t \epsilon_{kl}^t} K_{ij,kl}^t \right] F_{l,kl}^t = (\omega_l^t)^2 F_{l,ij}^t,$$

where i, j and k, l denote particle-hole pairs [15] and ϵ_{ij}^t the corresponding KS orbital energy differences. The coupling matrix is given by

$$K_{ij,kl}^t = \int d^3r_1 d^3r_2 \phi_{ij}^t(\mathbf{r}_1) \phi_{kl}^t(\mathbf{r}_2) \\ \times [1/r_{12} + \delta(\mathbf{r}_{12}) \partial v_{xc}(\rho^t(\mathbf{r}_1)) / \partial \rho^t(\mathbf{r}_2)],$$

with the GS electron density ρ^t , the product of two (real)

KS orbitals ϕ_{ij}^t , and the LDA exchange-correlation potential v_{xc} . The oscillator strength (OS)

$$f_I^t = \frac{4}{3} \sum_{\nu=1}^3 \left| \sum_{ij} \int d^3r \phi_{ij}^t(\mathbf{r}) r_{\nu} \sqrt{\epsilon_{ij}^t} F_{I,ij}^t \right|^2 \quad (1)$$

corresponding to the transition energies ω_I^t was accumulated in bins of width $\Delta\omega = 0.025$ eV yielding the absolute photoabsorption cross section per valence electron

$$\sigma(\omega) = \frac{1}{n-1} \frac{2\pi^2}{c} \frac{1}{t_s} \int_0^{t_s} dt \frac{1}{\Delta\omega} \sum_{I, \omega_I^t \in [\omega, \omega + \Delta\omega]} f_I^t.$$

We note first the overall good agreement between the magnitudes and shapes of the calculated and measured photoabsorption cross sections (shown here for Na_n^+ , $n = 3, 5$, and 9); compare the red histograms with the black curves in Fig. 1, and note that neither (artificial) numerical broadening nor a renormalization of the spectra has been applied. The slight deviations in peak positions are within the known accuracy of the TDLDA (± 0.2 eV) [10].

The calculated Na_3^+ spectrum at $T \approx 100$ K (Fig. 1a) exhibits a low energy peak originating [16] from two transitions $\omega_1^t = \omega_2^t \approx 2.65$ eV, from the occupied s -like orbital to two empty p -like KS orbitals located in the plane of the Na_3^+ equilateral triangle (see grey insets 1, 2, and 3 at the left of Fig. 1a). The high energy peak at $\omega_3^t = 3.41$ eV is due to an excitation to another p -like orbital that is perpendicular to the cluster plane (grey inset 4 in Fig. 1a). In the experiments $\sigma(\omega)$ is determined from the depletion of the Na_n^+ intensity due to dissociation following absorption of a photon $\hbar\omega$. Excitation into the *in-plane* antibonding orbitals (insets 2 and 3) promotes such dissociation and is accompanied by exhaustion of the OS for the first (lower energy) measured peak. Excitation into the *out-of-plane* orbital (inset 4) has no direct destabilizing effect and consequently in the measurements only 66% of the Thomas-Reiche-Kuhn sum rule (TRK) [10] is observed while the full TRK sum rule is found in the theoretical spectrum shown in Fig. 1a (as well as in all the calculated spectra that we show here).

Thermal motions distort the D_{3h} symmetry of the Na_3^+ GS and the degeneracy of the low energy transitions ω_1 and ω_2 is lifted. Indeed, the evolution of $\delta\omega_{21}^t = \omega_2^t - \omega_1^t$ coincides with the temporal behavior of the standard deviation $\Delta_b^t = \sqrt{\sum_i (b_i^t - \bar{b}^t)^2} / 3$ of the three bond distances b_i^t (see Fig. 2a). Additionally, the mean bond distance \bar{b}^t is strongly anticorrelated with the mean frequency $\bar{\omega}_{12}^t = (\omega_1^t + \omega_2^t) / 2$ as well as with the position of ω_3^t (compare the solid line with the lower and upper dashed curves in Fig. 2b)—that is, an increase of the ionic density (decrease of \bar{b}^t) results in a blueshift of the entire spectrum. Thus, the spectral linewidth of Na_3^+ can be fully understood in terms of line splitting and spectral sweeping with the first caused by symmetry breaking (degeneracy lifting, mechanism I) and the latter by breathing vibrations of the cluster (density oscillations, mechanism II).

Similarly, the finite temperature dynamics of Na_5^+ distorts (even at $T = 100$ K) the optimal D_{2d} GS symmetry

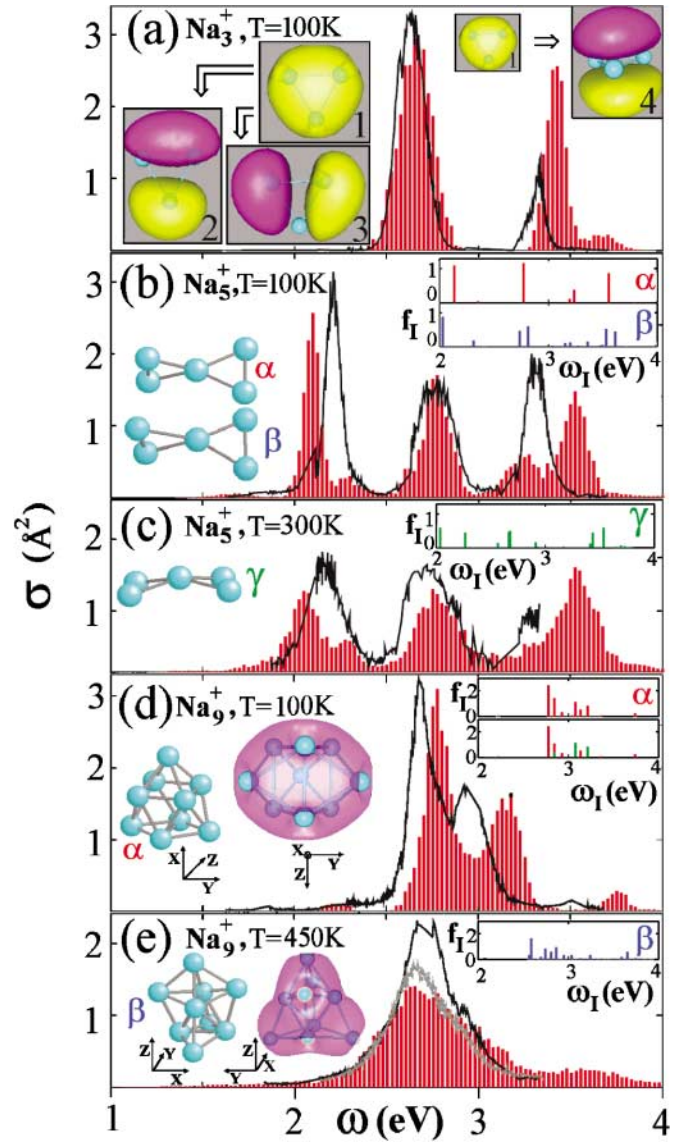


FIG. 1 (color). Theoretical (red histograms) and experimental [2] (black curves) photoabsorption cross section for Na_3^+ at 100 K (a), Na_5^+ at 100 K (b), and 300 K (c), as well as for Na_9^+ at 100 K (d) and at 450 K (e). Grey insets in (a) display isosurfaces of the four lowest KS orbitals where yellow and purple distinguish the sign of the wave function and light blue spheres mark the position of the ions. The top right corner insets in (b)–(e) show static TDLDA spectra: (b) for the Na_5^+ GS (structure α), and for an instantaneous structure β with an elongated left triangle; (c) for an instantaneous bent planar geometry (γ). The calculated spectrum shown in (d) derives exclusively from configurations lying in the basin of the GS structure α whose oblate spheroidal electron density is depicted by the purple isosurface. The static spectrum of α is shown in the top inset in (d), and in the bottom inset we show the decomposition of that spectrum into the component along the z axis (green sticks) and the perpendicular components (red sticks). The Na_9^+ isomer β is shown in (e), along with its electron density (purple isosurface) and its static spectrum (top right inset). To highlight the sensitivity of the experimental results to the temperature, we include in (e) the measured spectrum [2] at 540 K (grey curve).

(see GS α in Fig. 1b where the perpendicular left and right triangles are equivalent, and compare to the instantaneous structure β shown in Fig. 1b with an elongated left triangle), resulting in fragmentation (I) of the GS line at $\omega = 2.8$ eV into two spectral lines ω_u and ω_d [17] (compare red and blue lines in the upper right inset of Fig. 1b). The temporal variation of the absolute difference of the average bond lengths in the left and the right triangle ($\Delta_{lr}^t = |\bar{b}_l^t - \bar{b}_r^t|$, serving as a measure of the thermal structural distortion) correlates directly with the spacing $\delta\omega_{ud}^t = \omega_u^t - \omega_d^t$ between the frequencies of the spectral fragments (see solid and dashed curves in Fig. 2c).

While the relatively moderate structural distortions occurring at 100 K are not sufficient to lift the degeneracy of the states associated with the low energy absorption line of Na_5^+ (at ~ 2 eV, compare insets α and β at the upper right of Fig. 1b) which remains relatively sharp, increase of the temperature to 300 K results in bent configurations (see instantaneous structure γ on the left in Fig. 1c) where

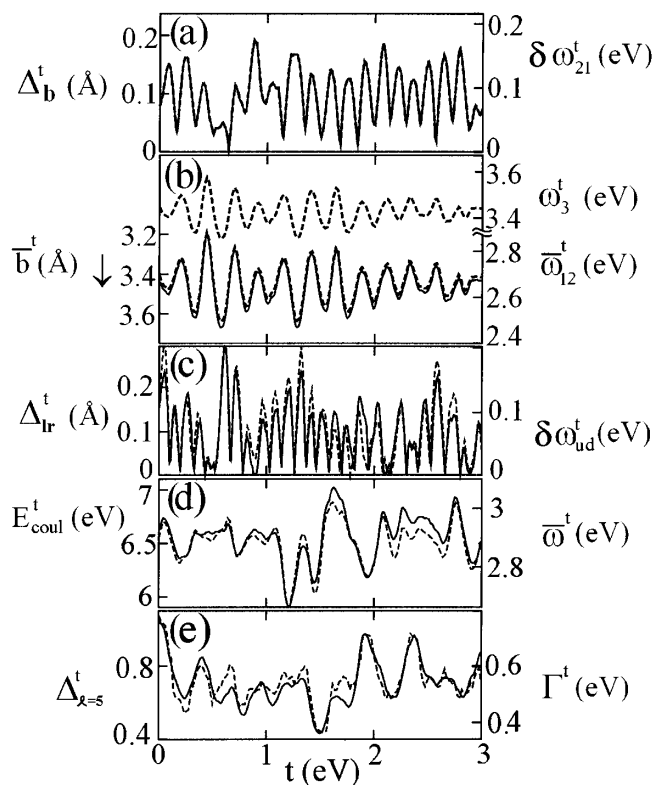


FIG. 2. Evolution of structural and spectral quantities with time: (a) the standard deviation Δ_b^t of the three Na_3^+ bonds (solid curve) coinciding with $\delta\omega_{21}^t$ (dashed curve) at 100 K; (b) the mean bond length \bar{b}^t of Na_3^+ (solid curve) and the mean frequency $\bar{\omega}_{12}^t$ (lower dashed curve), as well as the transition energy ω_3^t (upper dashed curve) at 100 K; (c) absolute difference $\Delta_{lr}^t = |\bar{b}_l^t - \bar{b}_r^t|$ between the average bond length in the left and the right triangle of Na_5^+ (solid curve) and $\delta\omega_{ud}^t$ (dashed curve) at 100 K; (d) interionic Coulomb repulsion per ion in Na_5^+ (solid curve) and mean energy of the corresponding TDLDA spectrum $\bar{\omega}^t$ (dashed curve) at 300 K; (e) $\Delta_{\kappa=5}^t$ (solid curve) and Γ^t (dashed curve) for Na_9^+ at 450 K.

the low energy line is fragmented (see inset γ at the upper right of Fig. 1c), resulting in enhanced broadening of that spectral line (compare Figs. 1b and 1c). Further broadening of the lines is caused by the aforementioned breathing modes (spectral sweeping mechanism II) reflected in the direct correlation between the interionic Coulomb repulsion E_{coul}^t (as a measure of the ionic density) and the average excitation energy $\bar{\omega}^t = \sum_l f_l^t \omega_l^t / (n-1)$ shown in Fig. 2d for the $T = 300$ K simulation.

For larger clusters, the occurrence of thermal isomerizations opens an additional line-broadening channel (III) [18]. The GS structure of the Na_9^+ cluster [19] is shown at the left of Fig. 1d (marked α) and the TDLDA spectrum calculated for this static configuration exhibits several absorption lines distributed in a bimodal-like manner (see top inset at the upper right of Fig. 1d). This bimodality, which is in contradiction to the single-line spectrum predicted by the jellium model [5], originates from the “oblate shape” of the cluster with radii $R_z = 2.68$ Å along the D_{3h} symmetry axis (z in Fig. 1d) and $R_{xy} = 3.22$ Å in the xy plane (these radii were determined from the diagonalized moment of inertia of the ionic GS structure α). The total electron density (see purple isosurface in Fig. 1d) is almost an ideal oblate spheroid. A decomposition of the OS of the D_{3h} GS into a z [$\nu = 3$ term in Eq. (1)] and the xy contribution ($\nu = 1$ and 2 terms) shows clearly that, as expected [3], the smaller spatial dimension in the z direction is associated with a higher excitation energy (compare green and red lines in bottom inset at the upper right of Fig. 1d). The bimodal character of the 100 K photoabsorption spectrum is evident in both the measured and calculated spectra (Fig. 1d), with further broadening caused by thermal motions through line-fragmentation and breathing vibrations of the cluster (mechanisms I and II).

The main thermal effect observed in the spectra of Na_9^+ is the conversion of the low temperature (e.g., $T = 100$ K, Fig. 1d) bimodal spectrum to one with a single broad maximum at higher temperatures (e.g., 450 K, Fig. 1e). This change in the spectrum is caused mainly by transformations between the GS geometry (α , Fig. 1d) and the structural isomer β (see configuration on the left of Fig. 1e). The static spectrum of the β isomer is shifted to lower energies with respect to that of the GS (α) structure (compare top insets marked α and β at the upper right corners of Figs. 1d and 1e). Thus, the high temperature broad spectral feature (Fig. 1e) is due to contributions from both the α and β isomers to the phase-space trajectories generated by the Langevin MD simulation at 450 K [20].

The β isomer may be characterized as having an octupolar shape, reflected in the shape of the electron density shown in Fig. 1e (see purple isosurface). To analyze the spectral broadening caused by transitions (at high T) between the GS (α) and the β isomer (which involve changes in shape multipolarity) we calculate the dimensionless multipole shape parameters [21], $a_{\ell m} = [\sqrt{4\pi} / (3r_s^\ell n^{\ell/3+1})] \sum_{i=1}^n r_i^\ell Y_{\ell m}(\theta_i, \phi_i)$, where (r_i, θ_i, ϕ_i) are the polar coordinates of the i th ion with respect to the center of

mass of the cluster and r_s is the density parameter of bulk Na. We defined a parameter $\Delta_\ell = \sum_{\ell'=2}^{\ell} \sum_{m=-\ell'}^{\ell'} |a_{\ell',m}|^2$ that measures the deviation from sphericity due to the multipole modes up to the order ℓ . Figure 2e shows a remarkable correlation ($R^2 = 84\%$, see Ref. [22]) between $\Delta_{\ell=5}^t$ and the width Γ^t of the spectrum at time t [Γ^t is twice the standard deviation of $\sigma^t(\omega)$ for $2 \leq \omega \leq 3.5$ eV]. Furthermore, including in such analysis only quadrupole and octupole deformations (i.e., $\Delta_{\ell=3}^t$) results in a similar high value of $R^2(73\%)$, while limiting consideration to the quadrupole deformation alone (i.e., $\Delta_{\ell=2}^t$) yields a poor correlation ($R^2 = 19\%$) pointing to the strong influence of octupolar deformations on the optical response of metal clusters (even closed shell ones, i.e., Na_9^+). This confirms our conclusion pertaining to the importance of the isomerization mechanism (III) in explaining the thermal evolution of photoabsorption spectra (particularly at high temperatures).

In summary, we demonstrated that calculations of absolute photoabsorption cross sections using the TDLDA in conjunction with *ab initio* MD simulations allow first-principles quantitative description and interpretation of optical spectra measured for sodium cations at various temperatures. Spectral line fragmentation resulting from symmetry-breaking ionic motions that lift electronic level degeneracies, frequency shifts (spectral sweeps) of the entire spectrum due to symmetry-conserving breathing vibrations, and structural isomerizations are identified as the main thermal line-broadening mechanisms with the first two operative for the smaller cluster (Na_3^+ and Na_5^+) and all three for larger ones.

This work is supported by the U.S. DOE, the Deutsche Forschungsgemeinschaft (M.M.), and the Academy of Finland (H.H.). We thank R.N. Barnett for discussions. Computations were done on Cray T3E at NERSC Berkeley and NIC Jülich.

-
- [1] W.A. de Heer *et al.*, Phys. Rev. Lett. **59**, 1805 (1987); C. Wang *et al.*, Z. Phys. D **19**, 13 (1991); C. Brechignac *et al.*, Chem. Phys. Lett. **164**, 433 (1989).
 [2] M. Schmidt *et al.*, Phys. Rev. B **59**, 10 970 (1999).
 [3] W. Ekardt, Phys. Rev. Lett. **52**, 1925 (1984); W. Ekardt and Z. Penzar, Phys. Rev. B **43**, 1322 (1991).
 [4] J.M. Pacheco *et al.*, Phys. Rev. Lett. **61**, 294 (1988).
 [5] C. Yannouleas *et al.*, Phys. Rev. Lett. **63**, 255 (1989).
 [6] G.F. Bertsch and D. Tomanek, Phys. Rev. B **40**, 2749 (1989).

- [7] V. Bonacic-Koutecky *et al.*, J. Chem. Phys. **104**, 1427 (1996).
 [8] G. Onida *et al.*, Phys. Rev. Lett. **75**, 818 (1995); A. Rubio *et al.*, Phys. Rev. Lett. **77**, 247 (1996); I. Vasiliev *et al.*, Phys. Rev. Lett. **82**, 1919 (1999).
 [9] J.M. Pacheco and W.D. Schöne, Phys. Rev. Lett. **79**, 4986 (1997); **81**, 5703 (1998).
 [10] M.E. Casida, in *Recent Developments and Applications in Modern Density-Functional Theory*, edited by J.M. Seminario (Elsevier, Amsterdam, 1996), p. 391.
 [11] V. Kresin, Phys. Rev. Lett. **81**, 5702 (1998).
 [12] R. Barnett and U. Landman, Phys. Rev. B **48**, 2081 (1993).
 [13] J.P. Perdew *et al.*, Phys. Rev. Lett. **77**, 3865 (1996).
 [14] N. Troullier and J.L. Martins, Phys. Rev. B **43**, 1993 (1991). The core radii (in units of a_0) are $s(2.45)$ and $p(2.6)$, with p as the local component. A plane-wave basis with a 10 Ry cutoff was used.
 [15] The convergence of $\sigma(\omega)$ with respect to the size of the computational cell ($48a_0$ in all three dimensions), and the number of orbitals (30–60) has been carefully checked.
 [16] For the smallest clusters (Na_3^+ and Na_5^+) an analysis of the largest elements in $F_{I,ij}$ [see Eq. (1) and Ref. [10]] allows assignment of the particular particle-hole pairs (i, j) that make a dominant contribution to a certain optical line I . Such analysis is not fruitful for larger clusters whose level spectra are more dense.
 [17] The OS of the Na_5^+ 2.77 eV line stems mainly from the transition from the first occupied orbital (with an elongated s -like shape) to two degenerate orbitals spatially separated on one of the two triangles.
 [18] While in the text we focus our discussion on the larger cluster Na_9^+ and remark that isomerization broadening was found by us also for sodium Na_7^+ , where at $T = 300$ K we observed structural transitions between the D_{5h} pentagonal bipyramidal GS and a D_{6h} planar hexagonal isomer (lying 141 meV above the GS) resulting in a bimodal spectral maximum for $\omega \sim 2.4$ eV, in addition to a broad absorption peak at 3.5 eV (see Ref. [2]).
 [19] The Na_9^+ GS structure (a tricapped trigonal prism, α in Fig. 1d) is lower by 98 meV than the Na_9^+ GS reported in Ref. [7] and depicted as configuration β on the left of Fig. 1e (a bicapped bipyramide with a C_{2v} symmetry).
 [20] Simulations of Na_9^+ at 450 K show a direct correlation between the ionic repulsion energy and the mean absorption frequency (similar to that shown in Fig. 2d for Na_5^+). The line broadening due to the breathing mode (mechanism II) implied by such correlation contributes merely 66 meV to the total width (~ 0.6 eV, see Fig. 1e).
 [21] M. Koskinen *et al.*, Z. Phys. D **35**, 285 (1995).
 [22] The coefficient $R = (1/t_s) \int dt [x(t) - \bar{x}][y(t) - \bar{y}] / (s_x s_y)$ is a common measure of the correlation between two time series $x(t)$ and $y(t)$ with means \bar{x} and \bar{y} and standard deviations s_x and s_y , respectively.